

Spaceborne Rainfall Doppler radar measurements: Correction of errors induced by pointing uncertainties

Eastwood Im^a, Simone Tanelli^a, Roberto Mascelloni^b, Luca Facheris^b

^a Jet Propulsion Laboratory, California Institute of Technology, Pasadena CA, USA

^b Dipartimento di Elettronica e Telecomunicazioni, Università di Firenze, Firenze, Italy

ABSTRACT

In this paper we present a sea surface radar echo spectral analysis technique to correct for the rainfall velocity error caused by radar pointing uncertainty. The correction procedure is quite straightforward when the radar is observing a homogeneous rainfall field. On the other hand, when NUBF occurs and attenuating frequencies are used, additional steps are necessary in order to correctly estimate the antenna pointing direction. The proposed method relies on the application of Combined Frequency-Time (CFT) technique to correct for uneven attenuation effects on the observed sea surface Doppler spectrum. The algorithm performance was evaluated by Monte Carlo simulation of the Doppler precipitation radar backscatter model, and the high-resolution 3D rain fields generated by a cloud resolving numerical model. Results show that the antenna pointing induced error can be successfully removed by the proposed technique.

Keywords: Spaceborne weather radar, Doppler

1. INTRODUCTION

Knowledge of the global distribution of the vertical velocity of precipitation is important in estimating latent heat fluxes, and therefore in the general study of energy transportation in the atmosphere. Such knowledge can only be acquired with the use of spaceborne Doppler precipitation radars. Although the high relative speed of the radar with respect to the rainfall particles introduces significant broadening in the Doppler spectrum, recent studies¹ have proven that the average vertical velocity in homogeneous rainfield can be measured to the 1 m/s accuracy level by appropriate selection of radar parameters at 14GHz. A suitable configuration for a nadir-looking Doppler precipitation radar (NDPR) is shown in Table 1. For inhomogeneous rainfall in which significant non-uniform beam filling (NUBF) takes place, the vertical velocity estimates are affected by a bias dependent on the along-track displacement of the 'center of mass' of the observed rainfield with respect to the actual satellite nadir. Such bias can be eliminated by our recently developed Combined Frequency-Time (CFT) processing technique². In this paper we deal with a further error introduced by the high relative speed v_s of the radar: the bias introduced by the off-nadir pointing angle.

Figure 1 shows the geometry of the problem and introduces the vector notation used throughout this paper. Specifically, \hat{i}_V is the unit vector in the antenna pointing direction, \hat{i}_x is the unit vector in the satellite motion direction (i.e., the along-track direction) and \hat{i}_z is the unit vector at nadir. Position vectors with respect to a fixed (ground) reference are represented as $\mathbf{p} = (x, y, z)$ in which the x- and z-axis of the Cartesian coordinate system are determined by \hat{i}_x and $-\hat{i}_z$, respectively. \mathbf{p}_s is the satellite position. Finally, $\mathbf{r} = (r, \theta, \phi)$ represents the positions with respect to the satellite (i.e., $\mathbf{r} = \mathbf{p} - \mathbf{p}_s$) where \hat{i}_V is the z-axis of the spherical coordinate system (i.e., $\theta = 0$). The center of the resolution volume is indicated by $\mathbf{r}_V = (r_V, 0, 0)$.

Using this notation, the radial velocity of a target at position \mathbf{p} and with velocity $\mathbf{u} = (u_x, u_y, u_z)$ can be written as:

$$v_r = v_s \hat{i}_x \cdot \mathbf{r}_V + v_s \hat{i}_x \cdot (\mathbf{r} - \mathbf{r}_V) - \mathbf{u} \cdot \mathbf{r} \quad (1)$$

where v_s is the satellite velocity. The three terms on right-hand side of (1) are the bias introduced by off-nadir pointing, the bias due to the target position relative to the center of the volume of resolution, and the actual radial velocity of the target, respectively.

*Simone Tanelli, Jet Propulsion Laboratory, M.S. 300-243 4800 Oak Grove Drive, Pasadena, CA 91109, U.S.A. E-mail: simone@radar-sci.jpl.nasa.gov

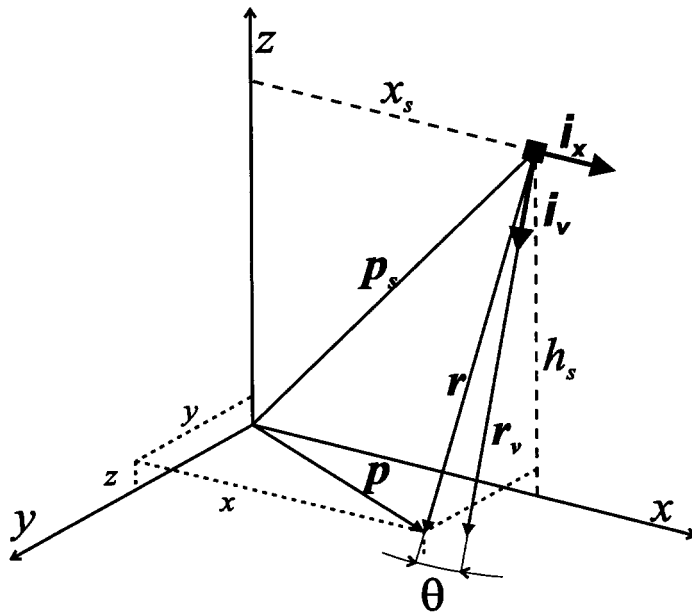


Fig. 1: Schematic of geometry of the problem. Generic point is indicated either by p or r : $p = (x, y, z)$ is relative to fixed cartesian system with x axis in along-track direction i_x , $r = (r, \theta, \phi)$ is relative to spherical coordinate system centered on satellite and with $\theta=0$ along radar pointing direction i_v . Satellite position is $p_s = (x_s, 0, h_s)$.

Satellite speed	v_s	7 km/s
Satellite altitude	h_s	432 km
Pulse repetition frequency	PRF	6000 Hz
Operating frequency	f_c	13.6 GHz
Operating wavelength	λ	2.2 cm
Nyquist Doppler velocity	v_m	$\lambda PRF/4 = 33$ m/s
Doppler shift rate	q_{zv}	$v_s/h_s = 16.2$ m/s km ⁻¹
Antenna diameter	D	5 m
3dB antenna beamwidth	θ_3	0.3°
"Null-to-null" beamwidth	θ_0	0.75°
Number of pulses	M	64
Number of samples per target track	M_β	$\text{Min}\{M, (2v_m/q_{zv})/v_s\}$
Minimum detectable rain reflectivity	N	17 dBZ

Table 1: Spacecraft and radar configuration parameters

$0.001^\circ \cong 4$ arcsec which corresponds to less than $\theta_3/100$. A pointing knowledge error $\theta_\alpha = 4$ arcsecs for a LEO satellite poses a serious technological challenge even for the most sophisticated ADS^{3,4,5,6}.

The pointing stability can be defined as an angle bound within a given temporal window. A first pointing stability budget is defined by setting the maximum rms angle variation during the observation time. For NDP, M radar pulses are required to obtain one vertical velocity estimate, therefore the observation time is $T_i = M / PRF \cong 0.01$ s, where PRF is the Pulse Repetition Frequency. The variation in pointing-induced bias must be less than the Doppler resolution $\Delta v = PRF \lambda / 2 M \cong 1$ m s⁻¹ during T_i , therefore one has the condition that $\text{rms}(\theta_\alpha) \leq \sigma_\beta = \sigma_\alpha$ within $T_i = 0.01$ s. Pointing error sources are often modeled by their torque spectrum, which, in general, has a 'low-pass' shape⁷ (i.e., a given rms(θ_α) threshold is easier to achieve for a shorter time window). Therefore only the torque spectrum part above the cutoff

For NDP, the latter term corresponds to the average vertical rainfall velocity (reflectivity weighted). For a cross-track scanning radar (i.e., $i_v \cdot i_x = 0$) contributions from horizontal winds must be taken into account. The second term generates the aforementioned broadening of the Doppler spectrum (for homogeneous rainfields) and the NUBF-induced bias.

The first term in the right-hand side of (1) is the pointing-induced bias v_p , it is zero only if r_v lies in the cross-track plane. In general spaceborne atmospheric radars are nadir looking or cross-track scanning, therefore nominally this term can be neglected. However, in practice, several factors introduce an error in the pointing angle of the radar (e.g., attitude determination errors, thermal distortions of the antenna support, vibrations due to moving parts, slew, thermal flutter or thermal snaps). Typically, spacecraft pointing error budgets are expressed in terms of pointing control error, pointing uncertainty and pointing stability.

The pointing control error is the angle between the nominal (desired) and actual instrument pointing vectors. For an NDP, the pointing control budgets can be set at the same level as other non-Doppler spaceborne atmospheric radars (1/10 to 1/2 of the antenna 3dB beamwidth). In fact, the bias in vertical velocity estimates due to the presence of a known off-nadir pointing angle can be easily accounted for through (1).

The pointing uncertainty is the angle between the actual instrument pointing error and the pointing error estimated by the spacecraft attitude determination system (ADS). For NDP, the pointing uncertainty budgets should be much more stringent than those for non-Doppler radars. In fact, given a typical science requirement of 1 m s⁻¹ accuracy in rainfall vertical velocity estimates, one could impose the unknown portion v_α of the pointing-induced bias not to exceed 1 m/s, e.g. $\text{rms}(v_\alpha) \leq \sigma_\alpha = 0.15$ m s⁻¹ in order to have a peak-to-peak error of . For a Low Earth Orbiting satellite $v_s \cong 7$ km s⁻¹, therefore a bias up to σ_α can be obtained for a pointing angle $\theta_\alpha = \arcsin(\sigma_\alpha / v_s) \cong$

frequency $f_l = 1/T_l$ has an impact on the pointing stability, whereas the whole spectrum contributes to the pointing error. For the pointing stability threshold σ_β introduced above, only components at frequencies above 100 Hz are to be taken into account. This pointing stability budget is less critical than that on pointing uncertainty since most error sources show spectra with dominant frequencies in the sub-Hz region.

A viable alternative to imposing very tight pointing knowledge error budget is to estimate the pointing-induced bias by analyzing the Doppler spectrum. In principle, assuming a circularly symmetric antenna pattern (here it is assumed Gaussian within the mainlobe), the ocean surface is expected to have zero vertical velocity when averaged over the radar footprint. If a non-zero vertical velocity is observed, that can be used to obtain the pointing-induced bias that should be removed from all vertical velocity estimates at the range cells above the surface. This approach is strictly related to the use of clutterlock procedures to determine the Doppler center frequency in SAR imaging⁸.

However one must take into account the attenuation that the radar pulse at 14 GHz undergoes while travelling through the rainfield. In fact, when NUBF occurs and medium to heavy rain rates are present, the surface return from different portions of the footprint is inhomogeneously attenuated and the measured surface Doppler spectrum can show a non-zero mean even if the pointing angle is precisely at nadir.

The NUBF induced distortion of the surface spectrum could be ignored by using only surface returns from clear air measurements adjacent to the observed rainy area, and interpolating them to obtain a the pointing-induced bias inside the rainy area. However, in this case one should impose a second, more stringent, pointing stability budget by considering an observation time equal to L_r / v_s , where the observation baseline L_r should be equal to the expected size of the largest rainfall event. For example, by setting $L_r = 100$ km, one should increase pointing stability requirements by imposing a maximum rms for pointing stability error sources above $v_s / L_r \cong 0.07$ Hz to be less than θ_α .

In this paper we propose to apply CFT to sea surface Doppler spectra in order to overcome the effects of NUBF-induced biases on surface vertical velocity measures, and therefore have a more frequent update of the estimated pointing-induced bias. By doing so, the baseline L_r is reduced to $2v_m/q_{rv} \cong 4$ km, and therefore the maximum rms of θ_α can be imposed only to pointing stability error sources above 1.75 Hz.

In this paper we analyze the impact of pointing errors on measurements of vertical velocity of rainfall through NDPR. In Section 2 a brief description of the pointing error budgets and the modeling of the pointing error are provided, in Section 3 a technique to correct for the pointing-induced bias on vertical velocity estimates is presented.

2. DOPPLER SPECTRUM OF THE SEA SURFACE

The Doppler spectrum of the sea surface for a narrow-beam radar pointing close to nadir can be expressed as:

$$P(x_s, \nu) = \int_{-\infty-\infty}^{+\infty+\infty} \int \eta(x, y; \nu - q_{rv} x') \cdot 10^{-0.2 \int k(x, y, z) dz} \cdot W_x(x - x_v) W_y(y - y_v) dx dy \quad (2)$$

where: $x' = r i_x$ is the along-track displacement from the zero Doppler *isodop* corresponding to the generic point on the surface $\mathbf{p} = (x, y, 0)$, q_{rv} is the Doppler shift rate, $\eta(x, y; \nu)$ is the sea surface natural Doppler velocity spectrum (*i.e.*, the sea surface spectrum that would be observed from a non moving, nadir looking, ideal instrument), $k(x, y, z)$ is the specific attenuation field in dB/km above the surface, $(x_v, y_v, 0)$ are the coordinates of the center of the footprint and $W_x(x)$ and $W_y(x)$ are the two way pattern weighting functions in the along-track and cross-track directions, respectively.

The natural Doppler spectrum can be also written as:

$$\eta(x, y; \nu) = \sigma_0(x, y) \cdot \eta_N(\nu) \quad (3)$$

where

$$\eta_N(\nu) = \frac{\eta(x, y; \nu)}{\int_{-\infty}^{+\infty} \eta(x, y; \nu) d\nu} \quad (4)$$

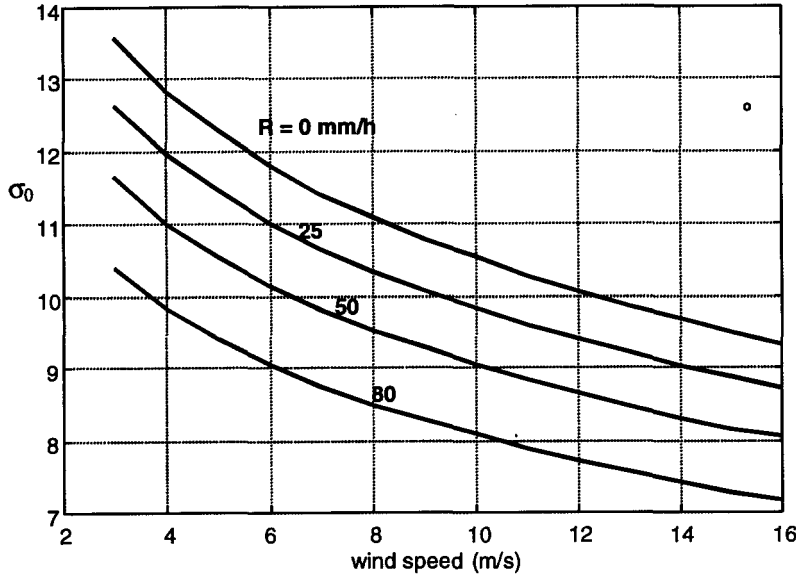


Fig 2. Normalized Radar Cross Section [dB] of the sea surface for a nadir pointing radar at 14 GHz as function of the wind speed at 20 m altitude and of the rain rate R at the surface. Results are calculated through a FWM e.m. model of the sea surface.

is the normalized natural Doppler spectrum and $\sigma_0(x,y)$ is the Normalized Radar Cross Section (NRCS). For NDPR $\eta_N(x,y;v)$ is much narrower than $W_X(x)$, therefore, if $\sigma_0(x,y)$ and $A(x,y) = 10^{-0.2 \int k(x,y,z) dz}$ are homogeneous within the footprint, the radar Doppler spectrum $P(x_s, v)$ is Gaussian and centered on $v_P = -q_{xy} x_V$. However, in general the NRCS depends on the radar frequency, incidence angle, wind speed at the surface w and rain rate at the surface R . For incidence angles close to nadir (e.g., less than 1 deg. off-nadir) the NRCS at 14 GHz varies by less than 0.1 dB depending on the angle. On the other hand, the dependence on R and w is significant. The results shown in Fig. 2 refer to a nadir looking radar at 14 GHz. They are derived from a Full Wave Model (FWM) ⁹ where the sea surface is characterized by the wind spectrum derived by Apel ¹⁰ and the ring waves generated by the raindrops. From these results we note that σ_0 decreases by increasing R (e.g., at nadir, σ_0 for a rain rate of 20 mm/hr is almost 1 dB below that with no rain).

The specific attenuation at 14 GHz is mainly determined by the rain rate R . Although no unique relationship exists between k (in dB/km) and R (in mm/hr), in general $k = a R^b$ where $a \sim 0.02$ and $b \sim 1.1$ ¹¹. It follows that larger R generate larger $A(x,y)$ and a lower $\sigma_0(x,y)$. These two effects combine together to modify the shape of the Doppler spectrum $P(x_s, v)$.

3. ESTIMATION OF THE POINTING ERROR

3.1 Estimation of sea surface apparent velocity through spectral moment estimators

The pointing-induced bias in vertical velocity measures v_P can be obtained by estimating the the first spectral moment of the sea surface Doppler spectrum $P(x_s, v)$. As long as a Gaussian spectrum is observed, several spectral moment estimators are available. The two most widely used in atmospheric weather radar applications are the Pulse Pair (PP) processing and the Discrete Fourier Transform (DFT) processing, elsewhere referred to as periodogram processing or spectral processing ¹². While the former provides better results for narrow spectra, the second performs better in the range of normalized spectral widths between 0.15 and 0.25 which is characteristic of spaceborne applications. In general, the variance of DFT estimates depends on the normalized spectral width w_N , on the number of samples M , on the signal to noise ratio SNR and on the parameter $A = (0.5 - v_{PN})/w_N$ where $v_{PN} = v_P / (2v_m)$. However, for NDPR in general $v_{PN} \ll 1$, since a minimum requirement for the ACDS is to provide a pointing error accuracy better than the antenna beamwidth. Therefore the variance can be approximated by ¹²:

$$\text{var}(\hat{v}_P) \approx \frac{(2v_m)^2}{M} \left[\frac{w_N}{4\sqrt{\pi}} + 2w_N^2 \frac{1}{\text{SNR}} + \frac{1}{12} \frac{1}{\text{SNR}^2} \right] \quad (5)$$

Furthermore, for spaceborne precipitation radars, $\text{SNR} \gg 10$ dB for the surface echo. Therefore we have that, in order to estimate v_P with a standard deviation of 0.15 m/s one needs $M \sim 4500$ which corresponds to an observation time of about 0.75 s and a baseline $L_r \sim 5.3$ km. This results in the capability of correcting for the bias induced by pointing error sources below 1.33 Hz.

The sensitivity of this method to the NUBF-induced deformation of the spectrum can be evaluated for a simplified case where $R(x,y,z) = R_f$ for $x > x_s$ and $z \leq H$; $R(x,y,z) = R_a$ for $x \leq x_s$ and $z \leq H$ and $R(x,y,z) = 0$ for $z > H$. By writing the

specific attenuation as $k = a R^b$ one obtains the total attenuation in the forward (A_f) and aft (A_a) halves of the footprint from:

$$A = 10^{-0.2HaR^b} \quad (6)$$

Under the assumption of a Gaussian antenna pattern the first moment of the spectrum for a nadir looking radar can be therefore written as:

$$v_p = q_{xy} \sqrt{\frac{2}{\pi}} \frac{h_s \tan(\theta_3/2)}{2\sqrt{\ln(2)}} (A_a - A_f) \cong 0.24 \cdot v_s \theta_3 (A_a - A_f) \quad (7)$$

Although (7) is derived from an extremely simplified model, it provides some quantitative reference to assess the impact of NUBF on antenna pointing correction through DFT spectral moment estimation of the sea surface echo. As an example, we note that, at 14 GHz, the parameters of the power-law can be approximated by: $a = 0.02$ and $b = 1.1$. Therefore even assuming $H = 2.5$ km (shallow rain), $R_a = 5$ mm/hr and $R_f = 8$ mm/hr (mild NUBF), one obtains a NUBF-induced bias $v_p = 0.7$ m/s on the vertical velocity estimate of the sea surface that would affect every spectral moment estimator¹.

3.2 Estimation of sea surface apparent velocity through Combined Frequency-Time technique

The CFT technique, described in² and briefly recalled here, aims at removing the NUBF-induced bias from the estimates of rainfall average vertical velocity by estimating the first moment of the tracks left by the rainfall distributed targets in the along-track satellite position / Doppler velocity ($x-v$) plane. Figure 3 shows a sequence of periodograms measured by a Doppler radar for a fixed range cell. Each periodogram is calculated from the DFT of a sequence of M complex voltage samples. Therefore one periodogram is obtained every M/PRF seconds which corresponds to an along-track

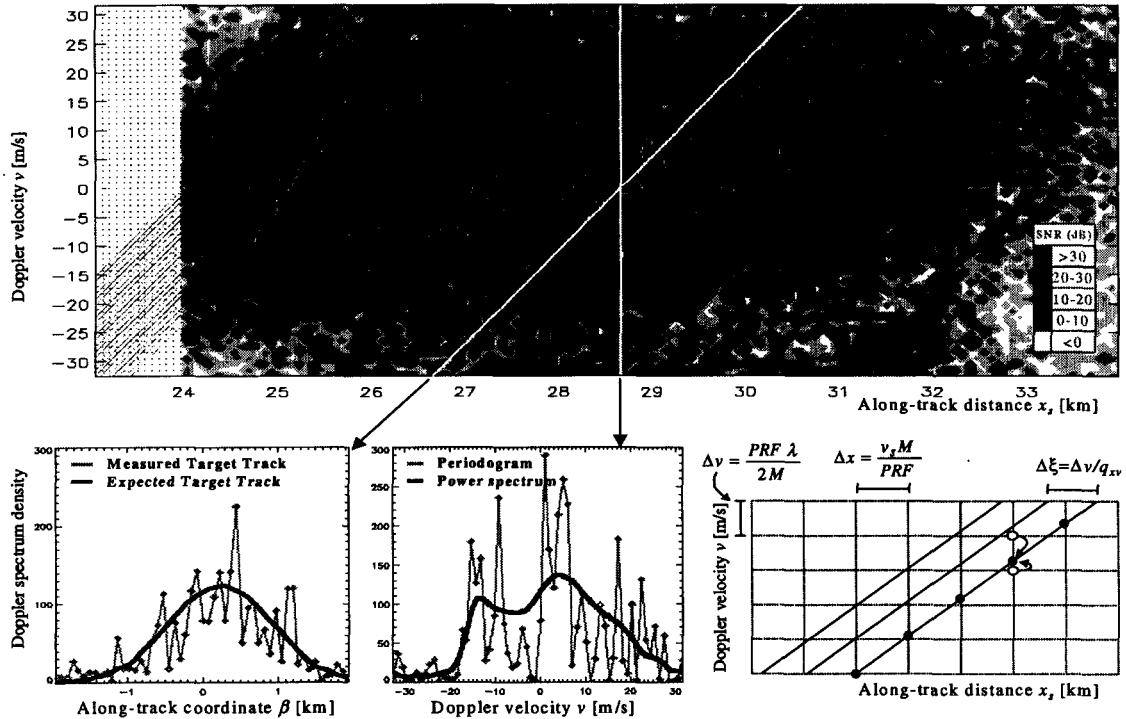


Fig. 3 Application of CFT to sequences of measured Doppler spectra: a) example of sequence of Doppler spectra, white diagonal lines indicate the target tracks, b) target track, c) periodogram, d) interpolation of power spectral samples to obtain measured target tracks.

displacement of the satellite $\Delta x = v_s M / PRF$. The example in Figure 3 is obtained from a typical NUBF situation where the power spectrum deviates significantly from a Gaussian shape. On the other hand, one can analyze the spectral density lines generated by a specific target at different times (i.e., the ‘target tracks’ along lines with slope $q_{xv} = v_s / h_s$ in the x - v plane). It has been demonstrated that for NDPR the target tracks can be well approximated by a Gaussian (from the shape of the antenna pattern), regardless of NUBF. Furthermore, the first moment of each target track indicates both the position when the target was in the antenna maximum gain direction, and the true vertical velocity of the target. Finally, a uniformly spaced horizontal profile of vertical velocity is obtained by using a weighted moving average of the target velocities obtained for each target track. The moving average ‘window’ is Gaussian shaped with width Δx which corresponds to a low-pass Gaussian filter with 3dB cutoff frequency $f_3 = v_s / (2\pi \Delta x)$.

The same procedure can be applied to remove the NUBF-induced bias from the spectrum of the sea surface. In fact, since $\eta_M(x, y; v)$ is narrower than the rainfall natural Doppler spectrum, the approximation of each target track with a Gaussian whose width is determined by the antenna pattern is even more accurate than for the rainfall application. It is important to note that such approach holds true only for small antenna beamwidths and small values of i_v, i_x , that is when the ‘cylindrical’ approximation used to calculate $A(x, y)$ is accurate.

4. SIMULATIONS AND RESULTS

Doppler spectra measured by NDPR have been obtained through a 3D Doppler radar simulator¹. The radar signal from the cells close to the surface accounts for the direct return from the sea surface and for the mirror image return. The radar signal of the sea surface is modeled as a Gaussian process because the size of the footprint (2.2 km) is much larger than the correlation length of sea surface roughness (up to 60 m for waves generated by winds up to 20 m/s, and few cm for rain-generated roughness). It is also assumed that the signal has zero-mean, in fact, even for small roughness of the sea surface (e.g., rms of height variation = 1 cm), the ratio between coherent and incoherent surface return is close to zero for a 14 GHz nadir-looking radar¹³.

The simulator was applied to 3D fields of hydrometeors and wind generated by a Cloud Resolving Model (CRM), and to 3D rainfall and vertical velocity fields measured by the NAS/JPL Airborne Rain Mapping radar¹⁴ (ARMAR). The spacecraft attitude errors were simulated by a stochastic process with cutoff frequency at 0.25 Hz.

Figure 4 shows the vertical section of a tropical squall line generated by the CRM initialized with soundings gathered during the TOGA/COARE measurement campaign. Figure 5 shows the corresponding along-track profile of the apparent velocity of the surface v_p (thick line), and its estimate obtained through DFT processing (thin) $v_{p(DFT)}$. In this case study $\langle v_p \rangle = -1.65$ m/s and $\sigma(v_p) = 0.25$ m/s over the whole temporal window. The reconstructed $v_{p(DFT)}$, if averaged out over the whole event, has a mean value $\langle v_{p(DFT)} \rangle = -1.74$ m/s, indicating that the dc component of the pointing uncertainty has been estimated satisfactorily. However, large errors affect $v_{p(DFT)}$ in areas where NUBF occurs.

In Figure 6 v_p is compared to the estimate $v_{p(CFT)}$ obtained through CFT processing of the sea surface echo. The results of four simulations performed on the same case study are shown by the four dash and dot lines. Overall, $\langle v_p - v_{p(CFT)} \rangle = 0.04$ m/s and $\sigma(v_p - v_{p(CFT)}) = 0.16$ m/s. This indicates that, CFT derived estimates are not biased and that also 60% the energy of error sources in the 0-0.5 Hz range has been accounted for. Estimated profiles $v_{p(CFT)}$ were obtained with the width Δx of the moving average window ranging between 3.5 and 10 km, which corresponds to a cutoff frequency between 0.15 Hz (dotted) and 0.5 Hz (dash dot). Among them, the error of estimates of v_p obtained with $\Delta x = 5$ km (which corresponds to the filter with cutoff frequency matching that of the pointing error process) showed the lowest standard deviation of 0.14 m/s.

Figure 7 shows a horizontal profile of rainfall vertical velocity v_R for the same event (thick) along with the estimated profiles $v_{R(CFT)}$ obtained through CFT processing with (thin) and without (dash) the correction for v_p as estimated by CFT processing of the sea surface. The following statistics were calculated: $\langle v_R - v_{R(CFT)} \rangle = 1.68$ m/s, $\langle v_R - v_{R(CFT)} - v_{p(CFT)} \rangle = 0.03$ m/s, $\sigma(v_R - v_{R(CFT)}) = 0.83$ m/s, $\sigma(v_R - v_{R(CFT)} - v_{p(CFT)}) = 0.8$ m/s. In general, the proposed method allows to attain unbiased estimates of vertical velocity of rainfall, with standard deviations < 1 m/s even in presence of NUBF and of pointing error sources below 0.25 Hz.

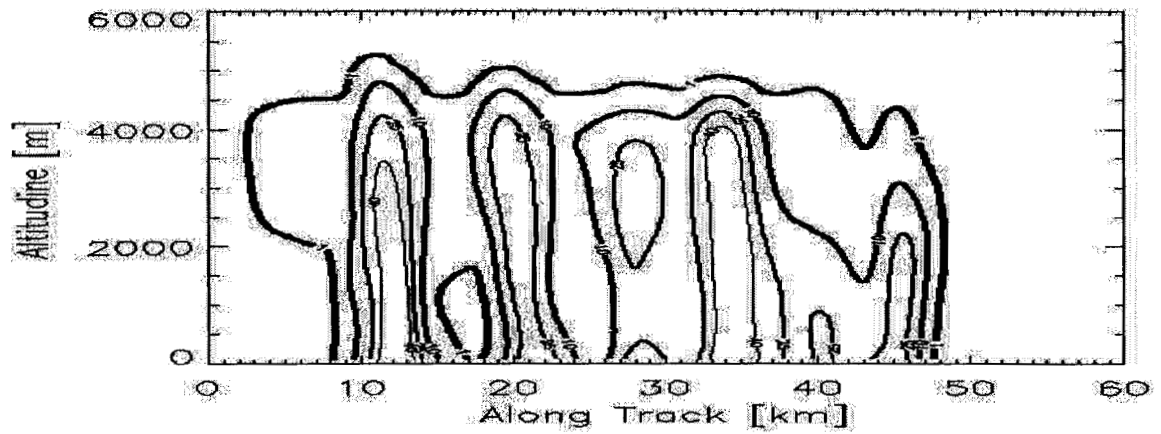


Fig. 4 – Vertical section of the rain rate field [mm/hr] of a tropical squall line along the satellite ground track.

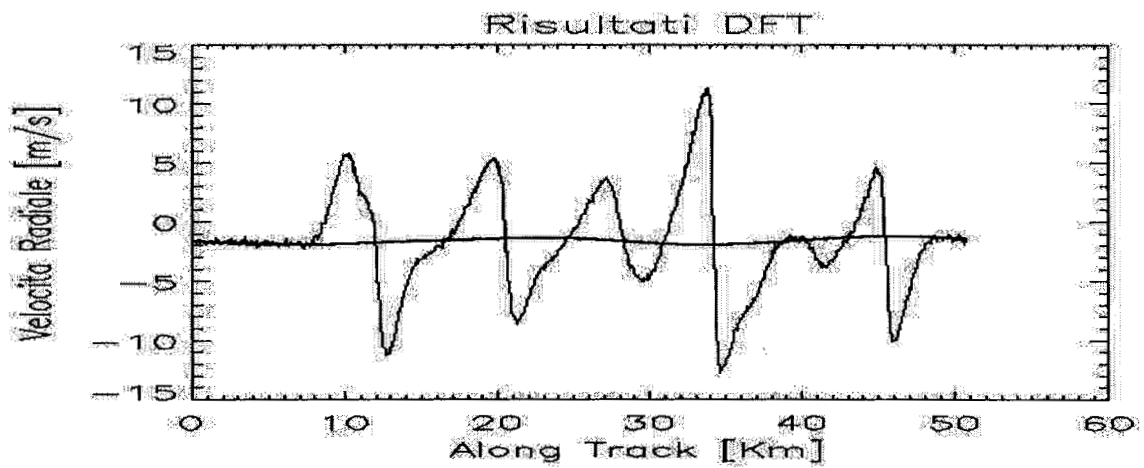


Fig. 5 – Vertical section of the rain rate field [mm/hr] of a tropical squall line along the satellite ground track.

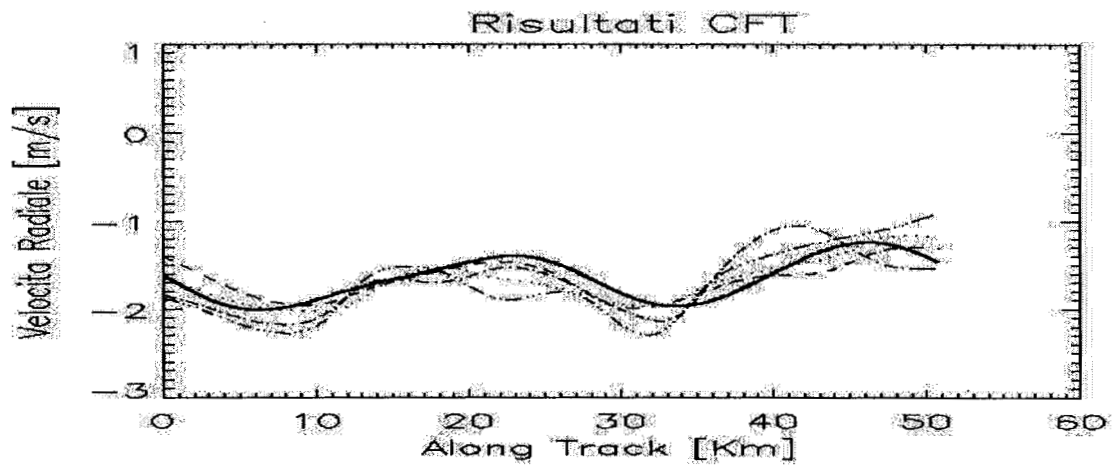


Fig. 6 – Vertical section of the rain rate field [mm/hr] of a tropical squall line along the satellite ground track.

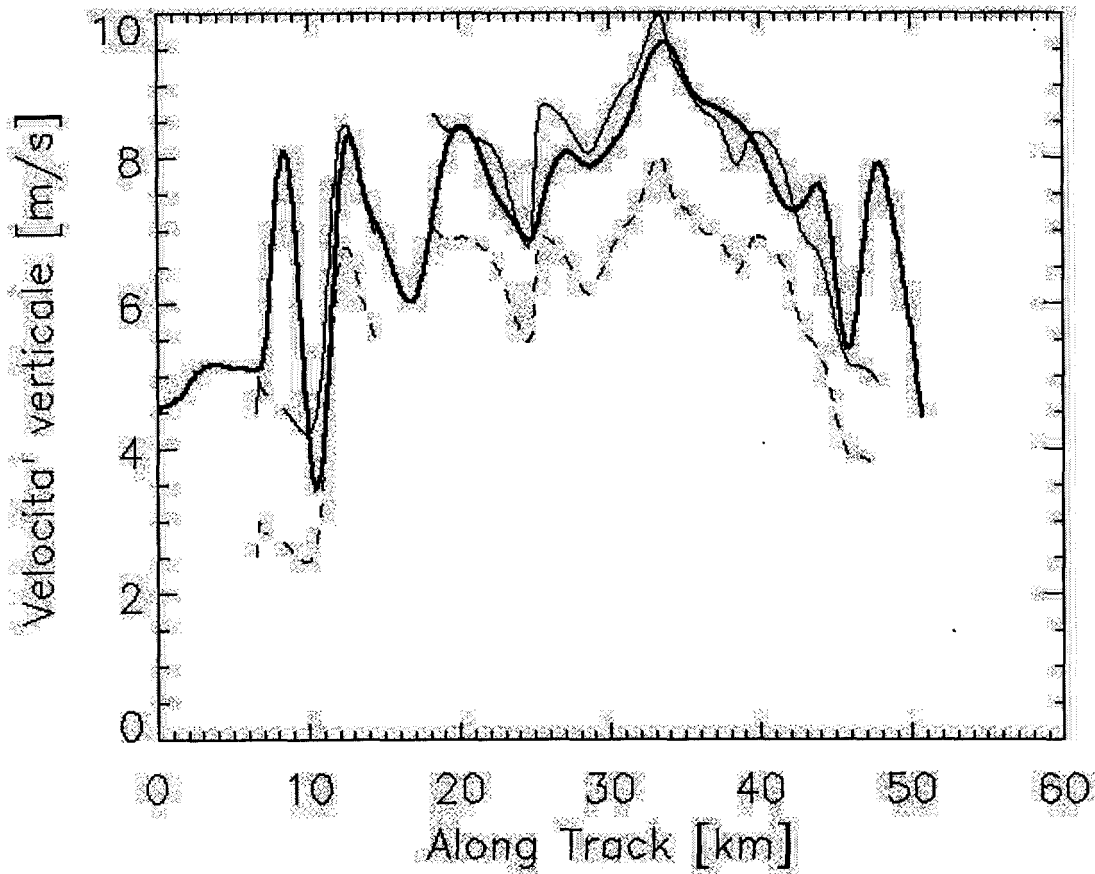


Fig 7. Along track profiles of rainfall vertical velocity: true (thick solid curve), estimated through CFT with no correction for the pointing angle (dashed curve), and estimated through CFT with correction for the pointing angle as estimated through CFT processing of the sea surface echo (thin solid curve).

5. CONCLUSIONS

Use of spaceborne Doppler radars in low earth orbit to monitor the vertical velocity of rainfall requires knowledge of the antenna pointing angle within few arcsecs. When such knowledge cannot be attained by the spacecraft Attitude Determination System, the estimation of the pointing-induced bias on estimates of rainfall vertical velocity can still be achieved by measuring the apparent sea surface velocity. When a homogeneous rainfall field is observed, the pointing induced bias is given by the first moment of the Doppler spectrum of the surface echo. However when NUBF occurs, and moderate to heavy rain rates are observed, the radar signal is not uniformly attenuated within the footprint. It follows that the first moment of the Doppler spectrum of the sea surface is a biased estimate of the pointing-induced error. This NUBF-induced bias can amount to several *m/s* for a LEO satellite.

Application of the Combined Frequency-Time technique to the sequence of measured Doppler spectra of the sea surface allows to correct for the NUBF-induced bias, and therefore to estimate correctly the pointing-induced bias and remove it from the rainfall vertical velocity estimates. In particular, the results shown in this paper show that CFT is effective in removing the low frequency components of the pointing error. Further investigation is needed to define the highest frequency of pointing error source that can be corrected by this approach.

6. ACKNOWLEDGEMENT

The research described in this paper was based on the work performed for the TRMM follow-on programs at the Jet Propulsion Laboratory, California Institute of Technology, under contract with the National Aeronautics and Space Administration, and at the University of Florence (Italy) through a program funded by the Italian Space Agency.

REFERENCES

1. S.Tanelli, E. Im, S.L.Durden, L. Facheris and D. Giuli, "The effects of nonuniform beam filling on vertical rainfall velocity measurements with a spaceborne Doppler radar". *J. Atmos. Oceanic Technol.*, **19**, pp. 1019-1034, 2001.
2. S. Tanelli, E.Im, L.Facheris, S.L.Durden, "Signal processing technique for removal of NUBF induced error in spaceborne Doppler precipitation radar measurements", Proc. of SPIE International Symposium on Remote Sensing – Remote Sensing of Clouds and the Atmosphere VI, Toulouse (F), Sept. 17 – 21, 2001, vol 4539, p. 221-232.
3. P. Sabelhaus et al., "On-orbit ACDS performance of the LandSat 7 spacecraft", *Adv. In the Astronautical Sci.*, **107**, pp. 685-695, 2001.
4. J.M. Sirota, P.Millar, E.Ketchum, B.E.Schutz and S.Bae, "System to attain accurate pointing knowledge of the geoscience laser altimeter", *Adv. In the Astronautical Sci.*, **107**, pp. 39-48, 2001.
5. C.Voth, L.K.Herman, C.M.Heatwole and G.M.Manke, "Attitude determination for the STEX spacecraft using virtual gyros", *Adv. In the Astronautical Sci.*, **107**, pp. 113-132, 2001.
6. J.R.Wertz and W.J.Larson, "Space Mission Analysis and Design". *Microcosm Press/Kluwer Academic Press*, 1999.
7. A.Y.Lee, J.W.Yu, P.B.Kahn and R.L.Stoller, "Space Interferometry Mission spacecraft pointing error budgets". *IEEE Trans. On Aerosp. And Electr. Sys.*, **38**, pp. 502-514, 2002.
8. Curlander J.C. and R.N. McDonough, 1991: *Synthetic Aperture Radar*, John Wiley and Sons, 657 pp.
9. Capolino, F., L. Facheris, D. Giuli, F. Sottili, "The Determination of the NRCS when Corrugated by Blowing Wind and Rainfall: an Application to Rainfall Rate Measurements Over the Sea". *ICAP, Int. Conf. Ant. Propagat., Edimburgh, UK, 14-17 April. 1997.*
10. Apel, J. R., "An improved model of the ocean surface wave vector spectrum and its effects on radar backscatter". *J. of Geophysical Research*, **99**, 16, pp. 269-16,291, 1994.
11. R. Meneghini and T. Kozu, "Spaceborne Weather Radar", *Artech House Ed.*, 1990, ISBN 0-89006-382-6
12. D.S. Zrnich', "Estimation of spectral moments for weather echoes", *IEEE Trans. On Geosc. Electr.*, **4**, pp.113-128, 1979.
13. A.Ishimaru, "Wave propagation and scattering in random media". *Academic Press*, 1978.
14. S.L. Durden, E. Im, F.K. Li, W. Ricketts, A. Tanner and W. Wilson, "ARMAR: An Airborne Rain-Mapping Radar". *J. Atmos. Oceanic Technol.*, **11**, pp. 727-737, 1994.